Science Arts & Métiers (SAM)

is an open access repository that collects the work of Arts et Métiers Institute of Technology researchers and makes it freely available over the web where possible.

This is an author-deposited version published in: https://sam.ensam.eu
Handle ID: .http://hdl.handle.net/10985/12465

To cite this version :

Christina BJERKEN, Axel STEUWER, Z WANG, J DANIELS, Jérôme ANDRIEUX, Jakob BLOMQVIST, Olivier ZANELLATO, Tuerdi MAIMAITIYILI - In situ observation of g-ZrH formation by X-ray diffraction - Journal of Alloys and Compounds - Vol. 695, p.3124-3130 - 2017

Any correspondence concerning this service should be sent to the repository Administrator : scienceouverte@ensam.eu

Arts et Métiers Institute of Technology

In situ observation of γ-ZrH formation by X-ray diffraction

T. Maimaitiyili [a, *], C. Bjerken [a], A. Steuwer [b], Z. Wang [c, d], J. Daniels [c], J. Andrieux [e], J. Blomqvist [a], O. Zanellato [f]

[a] *Materials Science and Applied Mathematics, Malmö University, Nordenskiöldsgatan 1, Malmö 20506, Sweden*
[b] *Nelson Mandela Metropolitan University, Gardham Avenue, 6031 Port Elizabeth, South Africa*
[c] *School of Materials Science and Engineering, UNSW Australia, Sydney, New South Wales 2052, Australia*
[d] *Australian Synchrotron, 800 Blackburn Road, Clayton, Victoria 3168, Australia*
[e] *European Synchrotron Radiation Facility, 6 rue J Horowitz, 38043 Grenoble, France*
[f] *PIMM, ENSAM CNAM CNRS, 151 Boulevard d l'Hopital, 75013 Paris, France*

A B S T R A C T

We report on the measurement of the formation of γ-ZrH during *in situ* gaseous charging. The measurements were undertaken using high-energy synchrotron X-ray diffraction. Experimental observation shows that γ-ZrH can form at 180 °C from a mixture of $\alpha+\delta$ while dehydrogenating at slow cooling rates. The observation is further supported by *ex situ* laboratory X-ray diffraction on deuterated Zr powder that has undergone a similar heat-treatment cycle. The crystal structure of γ-ZrH refinement agrees with the reported $P4_2/n$ structure found in the literature.

Keywords:
Zirconium hydride
γ-ZrH
Synchrotron X-ray diffraction
Hydrogen charging

1. Introduction

Zirconium (Zr) and Zr based alloys have been extensively investigated in the past half-century due to their wide-spread applicability in the nuclear power industry. Because of appreciable mechanical strength and high corrosion resistance at elevated temperature and pressure, good thermal conductivity and low thermal neutron absorption cross section, Zr based alloys can be used as fuel rod cladding material in the nuclear reactor core. It has been well known that the excess of hydrogen in Zr will degrade the mechanical properties of the material by forming Zr hydrides [1–4]. During reactor operation, the hydrogen in the surrounding environment will diffuse into hexagonal close packed (HCP) α-Zr matrix and later precipitate as Zr hydrides (ZrH_x, where x = H/Zr) once the hydrogen solid solubility limit is reached [1]. The formation of zirconium hydrides is considered to be a major cause of embrittlement; in particular, it is a key step in the mechanism of delayed hydride cracking.

The equilibrium phase diagram of zirconium-hydrogen (Zr-H) system is relatively complex, as the formation of different hydride phases is dependent on hydrogen concentration and cooling rate. Even today there is no clear agreement about the existing phases in the Zr-H system, position of the phase boundaries, stability of the hydride phases, phase transformation order and exact phase transformation temperature [5–7]. However, many authors [5–17] agree that the Zr-H system consists of at least two types of allotropic Zr phases, the HCP Zr phase known as α-Zr phase and the body centered cubic (BCC) Zr phase known as β-Zr; two stable hydride phases, the face centered cubic (FCC) Zr-hydride known as the δ-ZrH_x (x = 1.4–1.7) phase and the body centered tetragonal (BCT) Zr-hydride known as ε-ZrH_x (x = 1.75–2, c/a >1) phase; two metastable hydride phases, the face centered tetragonal (FCT) γ-ZrH_x (x = 1, c/a>1) phase with structure type ZrH, and one newly observed trigonal ζ- ZrH_x ($0.25 \leq x \leq 0.5$) [9] which seems to be fully coherent with the Zr matrix and is speculated to be a precursor of the δ- and γ-ZrH_x formation.

The type of hydrides formed in Zr based alloys and their morphology are determined by many factors, including purity of the Zr, heat treatment, external load, strain rate, cooling/quenching rate and hydrogen concentration [2,5,7–9,18]. In general, γ-ZrH tends to form as needle-like precipitates while the δ-Zr hydride forms with platelet-like morphology. In all three γ-, δ- and ε-Zr

* Corresponding author.
E-mail address: tuerdi.maimaitiyili@mah.se (T. Maimaitiyili).

hydrides, the hydrogen tends to occupy tetrahedral interstitial positions in the unit cell. Compared to commonly observed hydrogen rich BCT ε-ZrH_2 hydride, in which (nearly) all eight tetrahedral positions are fully (without loss of generality, we refer to it now as ε-ZrH_2) occupied by hydrogen, and non-stoichiometric FCC δ-Zr hydride, which has the same sites partially and randomly filled, the γ-ZrH has an ordered tetragonal unit cell with four hydrogen atoms on the tetrahedral sites of the (110) plane. According to some studies [19,20] the volume expansions caused by phase transformation of $\alpha \rightarrow \gamma$ and $\alpha \rightarrow \delta$ can reach as high as 12.3% and 17.2%, respectively. Hence, the precipitation of hydrides will introduce significant amount of misfit strain on the Zr matrix and reduces its ductility. The degree of degradation of various material properties of Zr-alloys after the formation of hydrides strongly depends on types of hydride, hydride orientation, distribution, quantity and morphology. Therefore, to push the limit and safely extend service lifespans of current and future nuclear reactors, understanding the problem of hydrogen absorption, hydride formation and subsequent phase transformations in zirconium alloys is significant.

2. Background

Although many studies have been carried out on γ-ZrH, there is still controversy regarding its stability, crystal structure, formation mechanisms, and the transformation temperature [5,21–24]. Most previous [8,25] literature report that the γ-ZrH is a metastable phase which has a tetragonal ($P4_2/n$) structure and forms normally upon fast cooling/quenching. [1]The γ-ZrH formation through normal/slow cooling has also been reported [27,28] based on neutron diffraction performed on deuterated commercial Zr-2.5 wt %Nb alloy samples. According to their observation the γ-ZrH phase is thermodynamically stable at room temperature, and there is a sluggish δ to γ-hydride transformation initiated at 180 °C during cooling. Similarly, Mishra et al. [29] also suggested that γ-ZrH is an equilibrium phase and there is a peritectoid reaction, from $\alpha+\delta$ to γ, occurring at about 250 °C. Such discrepancies may arise because of high diffusivity of hydrogen at low temperature, close structural similarities of various hydride phases, large stoichiometric range over which hydrides can form, strong influence of other impurity elements in the Zr-H system and also the sensitivity of the experimental methods. With the high temporal and spatial resolution of synchrotron X-ray diffraction (XRD), it is possible to detect a subtle and fast phase transformation in real time. Therefore, to overcome uncertainties produced by sample and instrument, an *in situ* hydrogenation experiment on commercial grade Zr-powder has been performed at the high energy synchrotron X-ray beamline ID15B at the European Synchrotron radiation Facility (ESRF), France. The formation and growth of γ-ZrH in commercial grade Zr powder was monitored in real time. In addition, the measurements on the same Zr powder deuterated to a concentration of Zr:H = 1:1 and heat treated *ex situ* in different condition were performed using laboratory X-ray instrumentation. The stable crystal structure and the evolution of the various phases have been studied by Rietveld [30,31] and sequential Pawley analysis, respectively. The study also demonstrated that the formation of the γ-ZrH does not necessarily depend on fast cooling rates as commonly stated. A manuscript with very similar conclusions but based on a different set of experimental data and observations using neutron diffraction has recently been submitted [32].

2.1. In situ hydrogenation

A commercial grade Zr powder with 99.2% purity was hydrogenated *in situ* using a high pressure/high temperature capillary system at beamline ID15B of the European Synchrotron Radiation Facility (ESRF) in Grenoble, France [33]. The Zr powder was filled into capillaries with diameter about 3 mm. In order to ensure good diffraction signal from the specimen and avoid gauge volume related problems, a beam of 0.4 mm × 0.4 mm which aligned to the center of the capillaries had been used for data collection and kept it fixed during measurements.

The hydrogenation started at 300 °C with static 0.5 bar hydrogen partial pressure until complete ε-ZrH_2 formation. After no further phase transformation was observed for about 3.5 h, the hydrogen and argon mixture supply were cut off and the temperature was raised until no more ε-ZrH_2 could be observed in the system. Then we start evacuating the system while heating. The temperature increase was stopped at 613 °C once the α-Zr phase started to form. Subsequently, the system was allowed to cool to room temperature at a cooling rate of 10 °C/min.

To capture all possible phase transformations that happened during hydrogenation and dehydrogenation, diffraction patterns were collected continuously throughout the measurement with an acquisition time of 2 s or 20 s. The positions of the data acquisition in time and temperature are shown in Fig. 1. However, to avoid any confusion, only the part of the whole thermal history curve of the hydrogenation studies which is relevant to the formation of γ-ZrH is shown in Fig. 2. All data in this period are collected with 20 s of acquisition time. Details about the sample processing and the measurements can be found elsewhere [34].

2.2. Laboratory X-ray diffraction

Deuterated Zr-powder as described in Ref. [32] with deuterium to Zr ratio 1:1 was filled into quartz capillaries inside a glove box under Ar atmosphere and placed into quartz Schlenk tubes. Then, dynamic pumping was used to evacuate any remaining Ar which may have been trapped inside the Schlenk tube. The packed powder was heated inside a furnace together with the Schlenk tube from room temperature (28 °C) to 500 °C at a heating rate of 10 °C/min. The sample was kept at 500 °C for 10 min and then allowed to cool to room temperature in air. In the end, the whole Schlenk tube with a heat-treated powder was placed into the glove box again

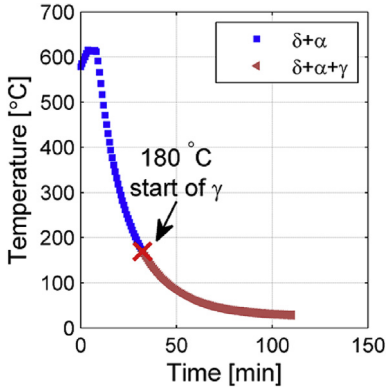

Fig. 1. Cooling curve of the *in situ* synchrotron XRD experiment. The position of the markers corresponds to where the data were acquired.

[1] Kolesnikov et al. 26. Kolesnikov, A.I. et al., *Neutron scattering studies of ordered gamma-ZrD*. Journal of Physics: Condensed Matter, 1994. **6**(43): p. 8977.; reported that the γ-ZrH belongs to the orthorhombic structure group and has a space group *Cccm*, but no other observation of this structure has been reported again to the best of our knowledge, and it will be disregarded from the discussion.

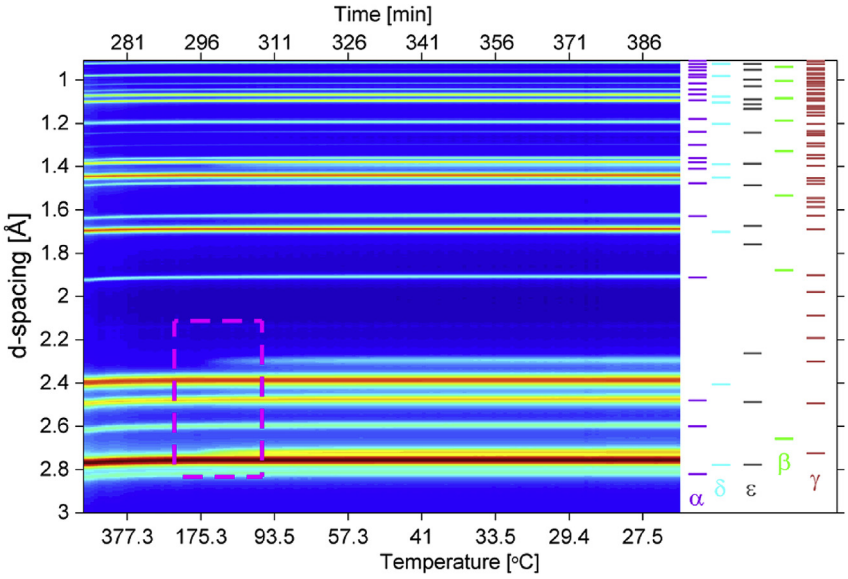

Fig. 2. Accumulated diffraction patterns from *in situ* hydrogenation studies. The color coded, small horizontal tick marks represents HKL peak positions of the labeled phases (right scale). β-Zr is index here for the to highlight its absence. (For interpretation of the references to colour in this figure legend, the reader is referred to the web version of this article.)

and the powder inserted in capillaries and sealed with wax for the X-ray measurements. To investigate the effect of different heating and cooling rates on the formation of γ-ZrH, other samples were prepared using similar procedures described above but with a lower heating rate (5 °C/min), shorter annealing time (6 min) and slower, furnace cooling. The details of the samples used for investigation were summarized in Table 1.

The laboratory XRD experiments were performed on a STOE diffractometer in transmission mode with copper radiation (λ = 1.540598 Å) in the 2θ range of 2–90°. The sample Lab2 was scanned for 10.5 h with an acquisition speed of 300 s/step; Sample Lab1 was scanned for 30 min with acquisition speed of 30 s/step, where step corresponds to 0.9° in 2θ. Here it should be noted that the deuterium and hydrogen are chemically indistinguishable, and hydrogen-deuterium replacement only marginally affects the diffusion rates and mobility of deuterium in the bulk zirconium sample [35]. However, the phase diagram of the Zr-deuterium system is same as the Zr-hydrogen system [36]. Thus, the knowledge regarding deuterium and hydrogen on hydride phase formation and transformation can be used to all intents and purposes in this study interchangeably. The only reason, deuterated zirconium samples were used for the laboratory X-ray diffraction studies compared with the counterparts with *in situ* hydrogen charging are the planned neutron diffraction studies. As deuterium has a larger coherent neutron scattering amplitude [37], it is more suitable for neutron diffraction studies.

2.3. Data processing and analysis

All diffraction patterns collected at different sources were analyzed with the structure analysis software package Topas-Academic [30] and the structure mentioned above and reported in literature. The wavelength and instrumental function for the *in situ* hydrogenation experiment were determined by refinement of a standard LaB_6 powder collected on the same setup. Peak profiles were modeled with a pseudo-Voigt profile function. To identify and confirm the existing phases at each distinct stable phase region before and after γ-ZrH formation, Rietveld refinements were performed for a selected number of patterns in each region. As the system is not in equilibrium during the phase transformation, the sequential Pawley refinements were carried out to follow the dynamics of the γ-ZrH lattice parameters during the γ-ZrH formation and growth. All refinements were performed on the full 2θ range available. The refinement parameters included the scale factor, unit cell parameters, background functions (Chebyshev) and zero errors.

Table 1
Details and labeling of the various samples.

Samples	H or D	Heating rate °C/min	Annealing time min	Cooling type
Lab1	D	5	5	Furnace
Lab2	D	10	10	Air
In situ RT	–	–	–	–
In situ 593	H	10	–	–
In situ RT*	H	10	5	±10

3. Results

The sections of recorded data from *in situ* de-hydrogenation studies which shows the formation of γ-ZrH as a function of temperature and time are shown in Fig. 2. The expected HKL peak positions of various phases in the Zr-H system are marked with color coded horizontal ticks at the right side of the figure. Although there are visible traces of Zr-oxide and other secondary phase reflections [38,39], for clarity their indices were not shown in this or other figures in the paper. For better visibility, the selected peaks in the diffractograms just before and after the formation of γ-ZrH enclosed with rectangle in Fig. 2 is shown in Fig. 3 as a waterfall plot.

One typical measured *in situ* data (in blue) collected at ESRF and its Rietveld fitting result (red) of the hydrogenated Zr powder at 29 °C after heat treatment, are shown in Fig. 4. The color coded vertical tick marks in the figure corresponds to HKL position of respective phases, and color codes are same with Fig. 2. The R_{wp} is 13.11%. The phase amounts obtained from this specific data of α, δ, and γ are, 11.14%, 80.81% and 8.03%, respectively. For simplicity, only the part of HKL indices of α, δ, and γ phase peaks which are not severely overlapped with each other are shown on top of each corresponding peaks (see Fig. 4).

As shown in Fig. 3, during *in situ* dehydrogenation process the γ-

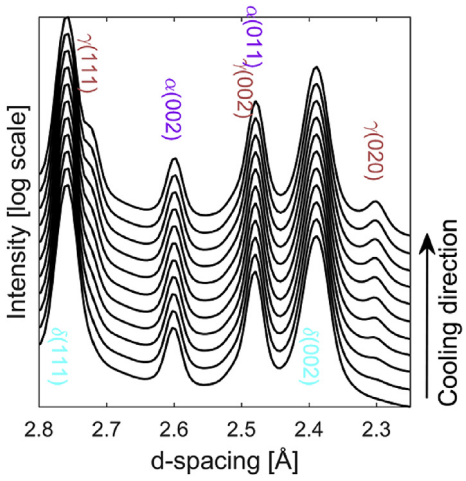

Fig. 3. A close-up on the area in Fig. 2 marked with a dashed rectangle on the intensity map, which illustrates the formation of γ-ZrH. For clarity some of the HKL indices are shifted slightly from it is exact position.

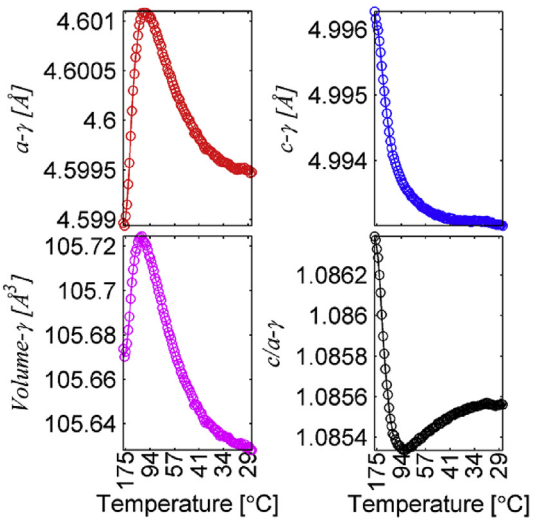

Fig. 5. The corresponding Pawley fitting result of γ-ZrH lattice parameter.

ZrH precipitated out from α+δ mixture, and no significant or sudden change of the temperature (recalescence) around γ-ZrH formation was observed. From both Figs. 2 and 3, one can see that the intensity of the γ-ZrH peaks increased with time following the reduction of hydrogen concentration. In order to observe any correlation between the temperature and evolution of the γ-ZrH unit cell parameters, *a*, *c*, volume and *c*/*a* of the γ-ZrH phase obtained from sequential Pawley refinements are presented in Fig. 5. It shows the expected decrease of the lattice parameters with cooling over time. The reason for the initial increase in lattice parameter '*a*' is unclear but can perhaps be attributed to the mismatch in volume and thermal expansion between γ-ZrH and the matrix during γ-ZrH formation, as well as a small change in composition. One typical Pawly fitting result (red) of the hydrogenated Zr powder at room temperature in the end of heat treatment (blue), is shown in Fig. 6. The color code of Fig. 6 is same with Fig. 4. As shown the calculated pattern agrees very well with observed data both graphically and statistically. The R_{wp} of the fit is 4.17%.

Fig. 7 shows a section of the diffraction patterns of deuterated Zr powder collected with laboratory X-ray source. The diffraction pattern in red (Lab 5 °C/min) is collected from a sample which was cooled in a furnace while the pattern in black (Lab 10 °C/min) is measured from a sample cooled in air.

Several selected diffractograms collected during *in situ* hydrogenation experiment and laboratory X-ray diffraction are compared in Fig. 8. As seen from the diffractograms labeled as *in situ* RT, in the beginning there is only α-Zr in the reference sample together with small amount of Zr-oxide and second phase particles. Later, the α-Zr phase will convert into a mixture of α+δ which is predominantly δ (labeled *in situ* 593 °C). Finally, at room temperature after hydrogen charging and some evacuation, some parts of the remaining α + δ phases transforms into γ. The final system consists of the phases: α, δ and γ (dataset *in situ* RT*). The diffractograms from two different heat-treated samples measured on a laboratory X-ray sources showed a similar composition of phases as the diffractogram *in situ* RT*.

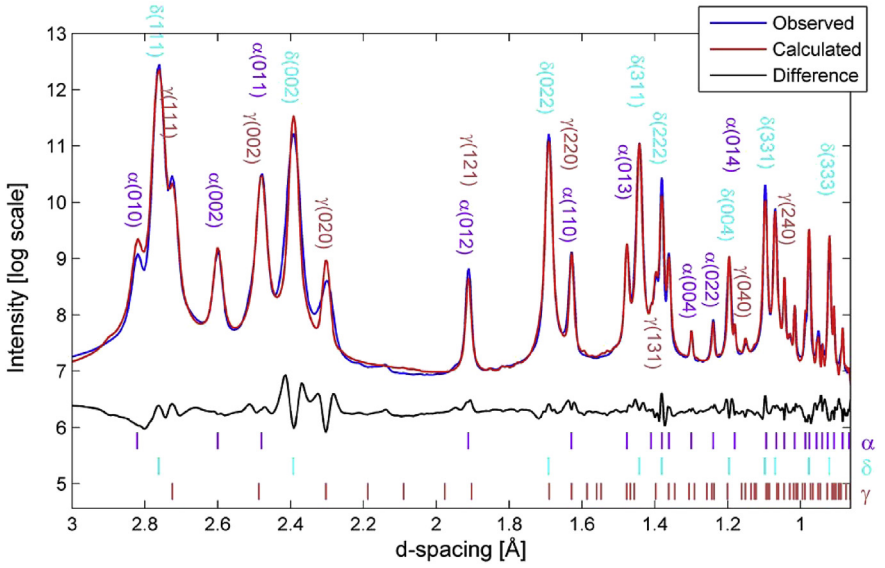

Fig. 4. Rietveld fitting result (red) from diffractogram collected (blue) at room temperature after dehydrogenation. Purple, cyan and brown vertical marks represents the peak position of α, δ, and γ phases respectively. (For interpretation of the references to colour in this figure legend, the reader is referred to the web version of this article.)

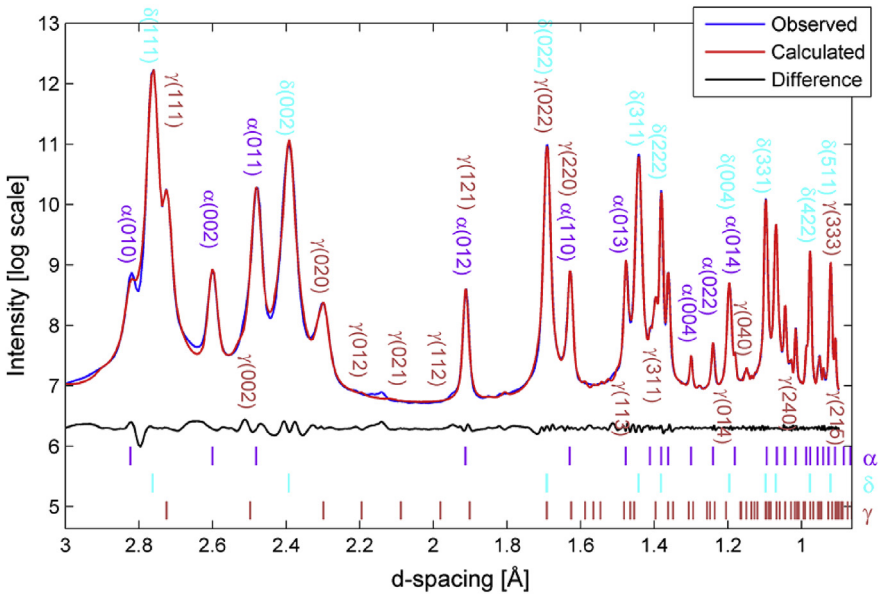

Fig. 6. Pawley fitting result (red) from diffractogram collected (blue) at room temperature after dehydrogenation. Purple, cyan and brown vertical marks represents the peak position of α, δ, and γ phases respectively. (For interpretation of the references to colour in this figure legend, the reader is referred to the web version of this article.)

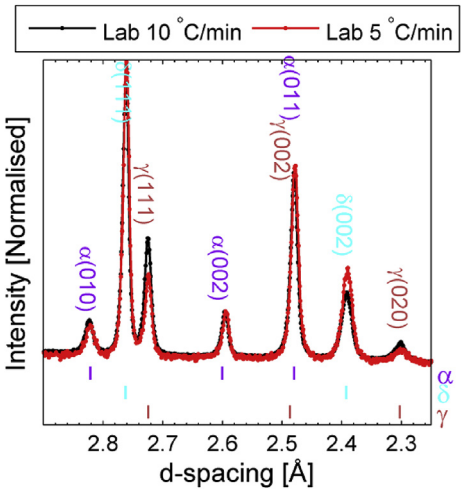

Fig. 7. The comparison of two different heat treated sample data measured by laboratory X-ray.

4. Discussions and conclusions

Utilizing the brilliance of synchrotron X-rays, the formation of the γ-ZrH has been recorded in real time. The good agreement between the experimental and calculated X-ray diffraction patterns in the Rietveld and Pawley refinements (*e.g.* Figs. 4 and 6) confirms the accuracy of the crystal structures and presence of hydride phases.

Both *in situ* and *ex situ* experiments together with their corresponding analysis showed that the γ-ZrH can form irrespective of the heat treatment rate (fast or slow) or time (short or long). It seems that, the formation of the γ phase in the Zr-H system is not strongly effected by heat treatment rates as commonly reported. Instead, it might be facilitated by the maximum annealing temperature which indirectly effects γ formation through changing the distribution, size and morphology of second phase particles in the system.

As shown in Figs. 2, 4, 6 and 8, there are traceable amount of monoclinic Zr-oxide present in the system during all measurements. At elevated temperature, the intensity of the oxide peaks increases slightly and later tetragonal Zr-oxide also becomes visible. However, all tetragonal Zr-oxide observed at high temperature dissolved at lower temperature during cooling cycles. Hence, it is possible that the amount of oxygen/oxide in the system might also have some effect on the stability of γ-ZrH in a similar way as it effects the boundaries between δ– and ε-ZrH observed in Refs. [5] and [17].

Previously [27,32], the presence of γ-phase was observed for extended periods of time at ambient conditions. This observation seems likely in our measurements also. However, none of the samples produced 100% γ-ZrH, in fact all are below 23%. As described in result section, the peak position of γ-ZrH varies according to expectation regarding the temperature decrease.

As noted in the *in situ* cooling curve of Fig. 1, prior to γ-ZrH formation there are both α and δ in the system from 610 °C to 180 °C. According to the equilibrium Zr-H binary phase diagram reported in Refs. [5,6], α and δ phase only coexist below 550 °C. The coexistence of α and δ phase at higher temperature maybe caused by α stabilizer present in the system.

The metastable transition phase ζ-ZrH_x reported in Refs. [8,9,40] has not been observed in any of the measurements here. However, the experimental evidence of the existence of metastable ζ- ZrH_x and possible transformation from ζ hydride to δ or γ hydride first reported by Zhao et al. [8,9] in 2008. Later in 2016, Schen et al. [40] not only show the presence of ζ hydride experimentally by using TEM, but they also did show the presence of transformation from δ to ζ hydride at 450 °C in contrast to this and other literature [1–7,22–29,32,34]. The possible reasons of not observing ζ hydrides maybe be related to (1) the presence of different impurity or alloying elements; (2) the formation and transformation rate of this phase might be much faster than the data acquisition rate; (3) the sensitivity of the instrument. In order to define the existence and transformation mechanism of the ζ phase to other hydride phases, more experiments needed with shorter data acquisition times and also different Zr and Zr-alloy samples.

The crystal structure of the γ-ZrH obtained from Rietveld and

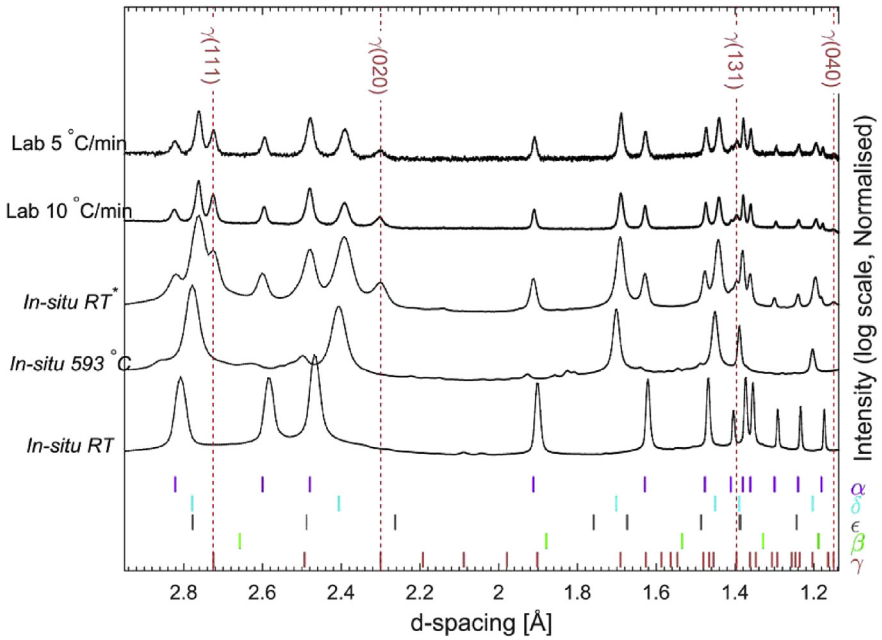

Fig. 8. Comparison of diffractograms collected on hydrogenated and deuterated samples collected at various instruments.

Pawley analysis agreed very well with reported space group of $P4_2/n$ structure with lattice parameters of $a = 4.5981$ Å, $c = 4.9954$ Å. The refined unit cell parameters a and c of α phase showed smooth variation with respect to temperature. The α-Zr unit cell parameters ($a = 3.2576$ Å, $c = 5.1998$ Å) observed at room temperature in all different measurements are slightly larger than these reported literature [5] values but difficult to ascertain as we have possible systematic uncertainties from the instrument, and the focus of the study was phase transformation not absolute structure determination. The lattice parameters of δ-ZrH_x obtained from both the Rietveld and Pawley refinements ($a = 4.7842$ Å) based on various measurements were found to be consistent with literature results [5].

To summarize, the precipitation of the γ-ZrH phase in high purity Zr-powder was examined *in situ* using high-energy synchrotron X-ray diffraction. Sequential Pawley analysis was carried out to study the dynamics of formation process. The present study showed the formation of γ-ZrH *in situ* at 180 °C from $\alpha+\delta$ mixture while slow cooling (during evacuation). The observations of this work is very useful for determining the stability and transformation mechanisms of the γ-ZrH. The γ-ZrH was also observed to form in *ex situ* laboratory X-ray diffraction experiments conducted on deuterated Zr powder with a similar heat-treatment, *i.e.* slowly heating at 5 °C/min and 10 °C/min and cooled in air or furnace, respectively for extended periods of time. The crystal structure of the γ-ZrH obtained from Pawley analysis agreed very well with reported space group of $P4_2/n$ with lattice parameters of $a = 4.5981$ Å, $c = 4.9954$ Å.

Acknowledgment

The ESRF is gratefully acknowledged for the provision of beam time under MA-1371. We are thankful to the Swedish Research Foundation (VR 2008-3844) for financial support. Professor S. Lidin at the Division of Polymer & Materials Chemistry at Lund University is gratefully acknowledged for providing access to his laboratory X-ray diffractometer and valuable discussion.

References

[1] R.N. Singh, et al., Terminal solid solubility of hydrogen in Zr-alloy pressure tube materials, J. Alloys Compd. 389 (1–2) (2005) 102–112.
[2] C.E. Ells, Hydride precipitates in zirconium alloys (A review), J. Nucl. Mater. 28 (2) (1968) 129–151.
[3] C.E. Coleman, D. Hardie, The hydrogen embrittlement of α-zirconium — a review, J. Less Common Metals 11 (3) (1966) 168–185.
[4] D.O. Northwood, U. Kosasih, Hydrides and delayed hydrogen cracking in zirconium and its alloys, Int. Met. Rev. 28 (1) (1983) 92–121.
[5] E. Zuzek, et al., The H-Zr (hydrogen-zirconium) system, Bull. Alloy Phase Diagr. 11 (4) (1990) 385–395.
[6] H. Okamoto, H-Zr (Hydrogen-Zirconium), J. Phase Equilib. Diffus. 27 (5) (2006) 548–549.
[7] L. Lanzani, M. Ruch, Comments on the stability of zirconium hydride phases in Zircaloy, J. Nucl. Mater. 324 (2–3) (2004) 165–176.
[8] Z. Zhao, et al., Characterization of zirconium hydrides and phase field approach to a mesoscopic-scale modeling of their precipitation, J. ASTM Int. 5 (2008) 15–33.
[9] Z. Zhao, et al., Identification and characterization of a new zirconium hydride, J. Microsc. 232 (3) (2008) 410–421.
[10] R.C. Bowman, et al., Electronic structure of zirconium hydride: a proton NMR study, Phys. Rev. B 27 (1983) 1474–1488.
[11] M.P. Cassidy, C.M. Wayman, The crystallography of hydride formation in zirconium: II the δ→ε transformation, Metall. Mater. Trans. A 11 (1) (1980) 57–67.
[12] B.W. Veal, et al., X-ray photoemission spectroscopy study of zirconium hydride, Phys. Rev. B 19 (1979) 2856–2863.
[13] W.M. Mueller, et al., Metal Hydrides, Academic Press, California, 1968.
[14] V.I. Ivashchenko, et al., Ab initio study of the electronic structure and phonon dispersions for TiH_2 and ZrH_2, in: Carbon Nanomaterials in Clean Energy Hydrogen Systems, Springer, Netherlands, 2008, pp. 705–712.
[15] J.S. Cantrell, et al., X-ray diffraction and nuclear magnetic resonance studies of the relationship between electronic structure and the tetragonal distortion in zirconium hydride (ZrH_x), J. Phys. Chem. 88 (5) (1984) 918–923.
[16] K.G. Barraclough, C.J. Beevers, Some observations on the phase transformations in zirconium hydrides, J. Nucl. Mater. 34 (2) (1970) 125–134.
[17] K.E. Moore, Phase relationships in the α+δ region of the Zr-H system, J. Nucl. Mater. 32 (1) (1969) 46–56.
[18] V. Perovic, et al., Hydride precipitation in α/β zirconium alloys, Acta Metall. 31 (9) (1983) 1381–1391.
[19] G.J.C. Carpenter, The dilatational misfit of zirconium hydrides precipitated in zirconium, J. Nucl. Mater. 48 (3) (1973) 264–266.
[20] A.T.W. Barrow, et al., Evaluating zirconium–zirconium hydride interfacial strains by nano-beam electron diffraction, J. Nucl. Mater. 432 (1–3) (2013) 366–370.
[21] B. Nath, et al., Effect of hydrogen concentration and cooling rate on hydride precipitation in α-zirconium, J. Nucl. Mater. 58 (2) (1975) 153–162.
[22] A. Steuwer, et al., Evidence of stress-induced hydrogen ordering in zirconium hydrides, Acta Mater. 57 (1) (2009) 145–152.

[23] M. Kerr, Mechanical Characterization of Zirconium Hydrides with High Energy X-ray Diffraction, PhD thesis, Mechanical and Materials Engineering, Queen's University, 2009.
[24] E. Tulk, et al., Study on the effects of matrix yield strength on hydride phase stability in Zircaloy-2 and Zr 2.5 wt% Nb, J. Nucl. Mater. 425 (1–3) (2012) 93–104.
[25] M. Ma, et al., Decomposition kinetics study of zirconium hydride by interrupted thermal desorption spectroscopy, J. Alloys Compd. (0) (2015).
[26] A.I. Kolesnikov, et al., Neutron scattering studies of ordered gamma-ZrD, J. Phys. Condens. Matter 6 (43) (1994) 8977.
[27] J.H. Root, R.W.L. Fong, Neutron diffraction study of the precipitation and dissolution of hydrides in Zr-2.5Nb pressure tube material, J. Nucl. Mater. 232 (1) (1996) 75–85.
[28] W.M. Small, et al., Observation of kinetics of γ zirconium hydride formation in Zr–2.5Nb by neutron diffraction, J. Nucl. Mater. 256 (2–3) (1998) 102–107.
[29] S. Mishra, et al., Formation of the gamma phase by a peritectoid reaction in the zirconium-hydrogen system, J. Nucl. Mater. 45 (3) (1972) 235–244.
[30] A. Coelho, Topas academic: technical reference, in: Topas Academic: Technical Reference, 2004. http://www.topas-academic.net/.
[31] A.C. Larson, R.B.V. Dreele, General Structure Analysis System (GSAS), 2000, 86–748.
[32] Z. Wang, et al., J. Alloys Compd. 661 (2016) 55–61.
[33] J. Andrieux, et al., A high-pressure and high-temperature gas-loading system for the study of conventional to real industrial sized samples in catalysed gas/solid and liquid/solid reactions, J. Appl. Crystallogr. 47 (1) (2014) 245–255.
[34] T. Maimaitiyili, et al., *In situ* hydrogen loading on zirconium powder, J. Synchrotron Radiat. 22 (2015).
[35] E.A. Gulbransen, K.F. Andrew, J. Electrochem. Soc. 101 (1954) 560–566.
[36] K.P. Singh, J.G. Parr, Trans. Faraday Soc. 59 (2256) (1963).
[37] V.F. Sears, Neutron News. 3 (1992) 26–37.
[38] K.T. Erwin, et al., Observation of second-phase particles in bulk zirconium alloys using synchrotron radiation, J. Nucl. Mater. 294 (3) (2001) 299–304.
[39] O. Zanellato, et al., Synchrotron diffraction study of dissolution and precipitation kinetics of hydrides in Zircaloy-4, J. Nucl. Mater. 420 (1–3) (2012) 537–547.
[40] H.H. Shen, et al., J. Alloys Compd. 659 (2016) 23.